# Power System State Estimation Considering Measurement Dependencies

Eduardo Caro, *Student Member, IEEE*, Antonio J. Conejo, *Fellow, IEEE*, and Roberto Mínguez

***Abstract*—State estimation measurements within a substation are routinely considered Gaussian and independent. In this paper the questionable independence assumption is dropped and a statistical procedure is proposed to estimate the measurement variance-covariance matrix. The well-known weighted least squares technique for estimation is then modified to take into account measurement dependencies. Two case studies are analyzed and conclusions duly drawn.**

***Index Terms*—Weighted least square, Dependent Gaussian measurements, Power system state estimation.**

## NOTATION

The main notation used throughout the paper is stated below for quick reference. Other symbols are defined as required in the text.

### A. Measurement

#### 1) Input Signals:

| | |
|---|---|
| $V_i^f$ | Voltage input measurement for bus $i$ and phase $f$. |
| $I_i^f$ | Current input measurement for phase $f$ for the generator/load of bus $i$. |
| $I_{ij}^f$ | Current input measurement for phase $f$ and line $ij$ at terminal $i$. |
| $\psi_i^f$ | Voltage-current phase angle input measurement for phase $f$ for the generator/load of bus $i$. |
| $\psi_{ij}^f$ | Voltage-current phase angle input measurement for phase $f$ and line $ij$ at terminal $i$. |

#### 2) Processed Measurement:

| | |
|---|---|
| $V_i$ | Voltage measurement for bus $i$. |
| $P_i$ | Active power injection measurement for bus $i$. |
| $Q_i$ | Reactive power injection measurement for bus $i$. |
| $P_{ij}$ | Active power flow measurement from bus $i$ to bus $j$. |
| $Q_{ij}$ | Reactive power flow measurement from bus $i$ to bus $j$. |

### B. Point Estimate Symbols

| | |
|---|---|
| $\eta$ | Number of input random variables. |
| $\nu$ | Number of output random variables. |
| $K$ | Number of the considered concentrations. |
| $\boldsymbol{p}$ | Input random variable vector. |
| $\boldsymbol{y}$ | Output random variable vector. |
| $p_{l,k}$ | Location of variable $p_l$ for concentration $k$. |
| $w_{l,k}$ | Weighting factor of variable $p_l$ for concentration $k$. |
| $\mu_{p_l}$ | Mean of random variable $p_l$. |
| $\sigma_{p_l}$ | Standard deviation of random variable $p_l$. |
| $\mu_{Y_q}^j$ | $j$-th non-cross moment of the random variable $y_q$. |
| $\sigma_{Y_q Y_{q'}}$ | Second centered cross moment between random variables $y_q$ and $y_{q'}$. |
| $\rho_{Y_q Y_{q'}}$ | Correlation coefficient between variables $y_q$ and $y_{q'}$. |

### C. State Estimation Symbols

| | |
|---|---|
| $n$ | Number of state variables. |
| $m$ | Number of measurements. |
| $r$ | Redundancy ratio of measurements. |
| $\boldsymbol{C}_z$ | Measurement variance-covariance matrix. |
| $\boldsymbol{W}$ | Weighting matrix of the traditional WLS estimator. |
| $\boldsymbol{z}$ | Measurement vector. |
| $\boldsymbol{e}$ | Measurement error vector. |
| $\boldsymbol{h}(\cdot)$ | Non-linear functional vector. |
| $\boldsymbol{c}(\cdot)$ | Non-linear equality constraint vector. |
| $\boldsymbol{g}(\cdot)$ | Non-linear inequality constraint vector. |
| $\boldsymbol{x}$ | State vector. |
| $\boldsymbol{x}^{\text{true}}$ | True state vector. |
| $\hat{\boldsymbol{x}}$ | Estimated state vector. |
| $\boldsymbol{r}$ | Residual vector. |

## I. INTRODUCTION

### A. Motivation

The aim of a state estimation procedure is estimating the state of a power system using a sufficiently large number of measurements of appropriate types and covering the whole power network. In addition to measurements, the structural data of the system are needed, i.e., topology, line/transformer parameters (resistances, reactances and shunt susceptances) and bus parameters (capacitor/reactance banks).

Measurement errors are routinely considered Gaussian-distributed and independent. We judge appropriate to consider measurement errors Gaussian, but generally inappropriate to consider them independent. Numerical simulations and field testing show that error distributions are reasonably Gaussian but they also show that measurement errors within a bus or a substation are clearly not independent. This is particularly so with current digital measurement systems that "fabricate" (active and reactive) power measurements out of "raw" measurements of voltage magnitudes, current magnitudes and current-voltage phase angles. Particularly, we consider that

E. Caro, A. J. Conejo, and R. Mínguez are partly supported by Junta de Comunidades de Castilla – La Mancha through project PCI-08-0102 and by the Ministry of Education and Science of Spain through CICYT Project DPI2006-08001.

Authors are with Univ. Castilla-La Mancha, Ciudad Real, Spain (e-mails: Eduardo.Caro@uclm.es, Antonio.Conejo@uclm.es, Roberto.Minguez@uclm.es)

voltage magnitudes, current magnitudes and phase angles are measured at each substation for each bus-bar and line, and then active/reactive power magnitudes computed electronically within the measurement system and transmitted to the Energy Management System (EMS), along with voltage measurements.

If statistical correlations among measurement errors are properly modeled and considered in the estimation procedure, a better estimate of the state of the system (i.e., closer to the true state) can be achieved. We show that this is actually the case and that taking into account measurement-error correlations makes a significant difference in terms of estimation quality.

### B. Aim

The aims of this paper are threefold. First, a technique is proposed to estimate efficiently the variance-covariance matrix of the measurement errors of all measurements in a substation. This technique is based on a well-know statistical procedure: point estimate. Second, an algorithm is provided to generate dependent measurements that are properly correlated according to a given measurement topology. Third, we propose a modification of the well-known Weighted Least Squares (WLS) estimation procedure that considers dependencies among measurements.

### C. Literature Review

The technical literature is rich in references pertaining to state estimation techniques and algorithms [1]–[11]. The pioneering work is due to Schweppe *et al.* [1]–[3] and others [4]. The model for the state estimation problem is well established, and diverse solution alternatives are also well known [8]–[11]. Particularly, [12] describes the preliminary design of a state estimator with dependent non-Gaussian measurements, which uses appropriate statistical transformations. Besides [12], not much work has been done so far on measurement dependencies. Reference [3] states that measurement correlations, which depend on the system state, should be considered. Some works also recognize that certain measurements such as voltage and active and reactive power injections at a given bus, for example, are correlated in both transmission and distribution networks [13]–[14]. Specifically, reference [15] studies the effect of considering different values of measurement variances on the estimations.

Nevertheless, emphasizing computational efficiency, measurement dependencies have been traditionally disregarded, which results in less accurate estimates [3],[15]. To the best of our knowledge, no references studying in detail the measurement dependencies applied to state estimation are available in the technical literature.

### D. Contribution

The contributions of this paper are: (i) to provide a state estimation technique that takes into account the dependencies among measurements within each substation as well as (ii) to derive an estimation procedure for the variance-covariance matrix of the measurement errors.

### E. Paper Organization

The rest of this paper is organized as follows. Section II characterizes the measurements within a substation, and provides a procedure to estimate the variance-covariance matrix of these measurements. Section III provides a WLS estimation algorithm that takes into account the dependencies among measurement errors. Section IV provides an algorithm to generate correlated measurements. Section V provides and analyzes results from two realistic case studies. Finally, Section VI provides some relevant conclusions.

## II. Measurement Dependency

### A. Measurement Structure

Each substation of a power system is equipped with electronic devices called Remote Terminal Units (RTU) that collect from the measurement system various types of measurements, usually active/reactive line power flows and bus voltages. These measurements are processed by the state estimator, which provides an optimal estimation of the system state based on the available measurements and on the assumed system model. Traditionally, all measurements are considered independent with zero-mean Gaussian errors [10].

In order to study the validity of this independency assumption, measurement topology and data processing should be considered. The connection of a typical three-phase multifunction meter is shown in Fig. 1 [16]. In this three-phase connection diagram, three voltage and three current signals are used as input data for the multifunction meter (see Fig. 2). This electronic device converts these analog signals into digital ones, processes them and provides the measurements (output data) that the state estimator uses. To compute each output measurement, the multifunction meter makes use of all the input data.

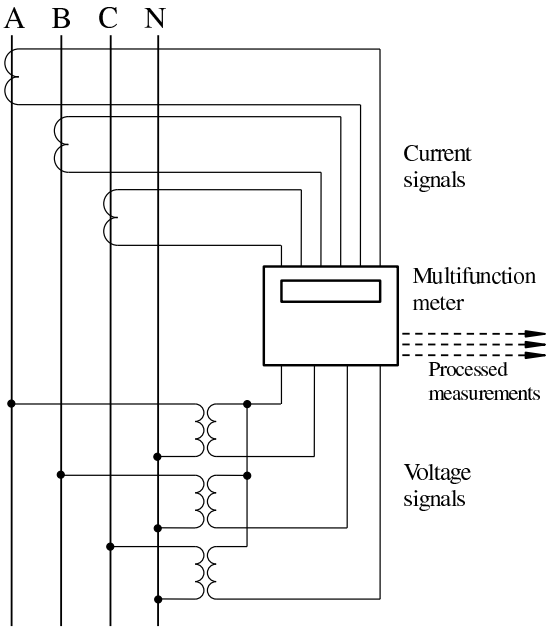


Fig. 1. Voltage and current signal connections in a three-phase measuring configuration.

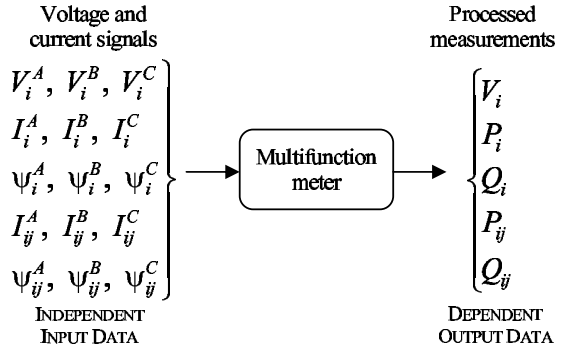


Fig. 2. Voltage and current signals, multifunction meter and processed measurements.

Dependencies between processed measurements can be represented by the measurement variance-covariance matrix for the whole power system, $\boldsymbol{C}_z$. Since there are no voltage-current signal connections between substations, processed measurements exhibit dependencies just between other processed measurements at the same substation. Therefore, matrix $\boldsymbol{C}_z$ is a diagonal blocked matrix, whose blocks $\boldsymbol{C}_{z,i}$ are the measurement variance-covariance matrices for each substation:

$$\boldsymbol{C}_z = \begin{pmatrix} \boldsymbol{C}_{z,1} & \mathbf{0} & \cdots & \mathbf{0} \\ \mathbf{0} & \boldsymbol{C}_{z,2} & \cdots & \mathbf{0} \\ \vdots & \vdots & \ddots & \vdots \\ \mathbf{0} & \mathbf{0} & \cdots & \boldsymbol{C}_{z,n} \end{pmatrix} . \quad (1)$$

In order to compute each $\boldsymbol{C}_{z,i}$ submatrix, the internal digital calculations of the multifunction meter should be considered. The following expressions correspond to the most relevant output measurements (for a three-phase connection configuration), assuming a sinusoidal system state (which is a typical assumption in state estimation) [16]:

$$V_i = F_{V_i}(\cdot) = \frac{V_i^A + V_i^B + V_i^C}{3} \quad (2)$$

$$P_i = F_{P_i}(\cdot) = \sum_{f=\{A,B,C\}} V_i^f I_i^f \cos(\psi_i^f) \quad (3)$$

$$Q_i = F_{Q_i}(\cdot) = \sum_{f=\{A,B,C\}} V_i^f I_i^f \sin(\psi_i^f) \quad (4)$$

$$P_{ij} = F_{P_{ij}}(\cdot) = \sum_{f=\{A,B,C\}} V_i^f I_{ij}^f \cos(\psi_{ij}^f) \quad (5)$$

$$Q_{ij} = F_{Q_{ij}}(\cdot) = \sum_{f=\{A,B,C\}} V_i^f I_{ij}^f \sin(\psi_{ij}^f) , \quad (6)$$

where $V_i^f$ is the voltage signal for phase $f$ and bus $i$, $I_{ij}^f$ and $\psi_{ij}^f$ are the current and voltage-current angle signals for phase $f$ and line $ij$ at terminal $i$, and $I_i^f$ and $\psi_i^f$ are the current and voltage-current angle signals for phase $f$ for the generator/load of bus $i$.

From (2)–(6), note that if an input signal contains a gross error, some output measurements are inaccurately computed. In other words, an input measurement error *propagates* through several output measurements, provoking multiple interacting bad data.

It is assumed that in a bus where more than one line is connected, voltage signals are shared between multifunction meters (see Fig. 3). On the other hand, if each multifunction meter has its own voltage and current signals, $\boldsymbol{C}_{z,i}$ becomes a blocked matrix itself. Some multifunction meters can be connected to two phases, and internal calculations differ from equations (2)–(6). Pursuing clarity and without loss of generality, in this paper it is assumed that all buses have a three-phase meter connection.

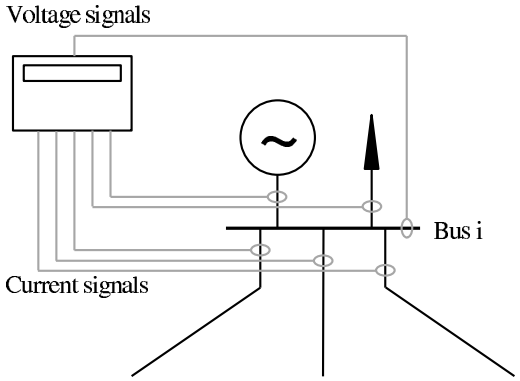


Fig. 3. Bus connecting more than two lines, and meter connection.

### B. Point Estimate

Point estimate methods are used to characterize statistically a set of $\eta$ output random variables of a problem, given some commonly known information about the statistical distributions of the set of $\nu$ random input variables.

Specifically, point estimate methods provides an estimation of the first moments of the output variable $\boldsymbol{y}$, which are defined as a function of the input variable vector $\boldsymbol{p}$, i.e., $\boldsymbol{y} = \boldsymbol{F}(\boldsymbol{p})$.

In our study, the input random variable vector $\boldsymbol{p}$ comprises all input signals,

$$\begin{aligned} \boldsymbol{p} &= [p_1, \ldots, p_l, \ldots, p_\eta]^T \\ &= [V_i^f, I_i^f, \psi_i^f\ I_{ij}^f, \ldots, I_{ik}^f, \psi_{ij}^f, \ldots, \psi_{ik}^f]^T , \end{aligned}$$

the output random variable vector $\boldsymbol{y}$ comprises all processed measurements,

$$\begin{aligned} \boldsymbol{y} &= [y_1, \ldots, y_q, \ldots, y_\nu]^T \\ &= [V_i, P_i, Q_i, P_{ij}, \ldots, P_{ik}, Q_{ij}, \ldots, Q_{ik}]^T , \end{aligned}$$

and the transformation functional vector $\boldsymbol{F}(\cdot)$, defined from (2)–(6), is:

$$\begin{aligned} \boldsymbol{F}(\cdot) &= [F_1(\cdot), \ldots, F_q(\cdot), \ldots, F_\nu(\cdot)]^T \\ &= [F_{V_i}(\cdot), F_{P_i}(\cdot), F_{Q_i}(\cdot), F_{P_{ij}}(\cdot), \ldots, F_{P_{ik}}(\cdot), \\ &\quad F_{Q_{ij}}(\cdot), \ldots, F_{Q_{ik}}(\cdot)]^T . \end{aligned}$$

The statistical information of each input variable ($p_l$) distribution is concentrated in $K$ pairs of numerical values, called *concentrations*. Each concentration is composed of a location, $p_{l,k}$ and a weight, $w_{l,k}$, whose expressions depend on the

considered point estimate algorithm.

Locations define the points in which functions $F_q(\cdot)$ are evaluated. The values of these evaluations ($Y_q(l,k)$) comprise information about the function $F_q(\cdot)$ and its influence on the output random variable $y_q$ distribution, but they have not any statistical interpretation. In order to weight the different influences, the weighting factors $w_{l,k}$ are used, but they can not be mathematically interpreted. Finally, moments of output variables are computed as a weighted sum of all the evaluations $Y_q(l,k)$.

Several point estimate methods have been proposed in the technical literature [17]–[24]. They mainly differ on the type of variables that they can deal with and on the number of evaluations of $\boldsymbol{F}(\cdot)$ to be performed. From among all of them, Hong's two-point estimate method [24]–[25] is used in this study for its simplicity and accuracy.

The point estimate algorithm is detailed below. The single underlying assumption considered is that input signals are considered Gaussian-distributed random variables, as detailed in Section II-A.

1) *Calculation of locations*: Locations $p_{l,k}$ $(k = 1, 2)$ are computed as follows (see [25]):

$$p_{l,1} = \mu_{p_l} + \sqrt{\eta}\sigma_{p_l} \quad , \quad p_{l,2} = \mu_{p_l} - \sqrt{\eta}\sigma_{p_l} \ , \tag{7}$$

where $\mu_{p_l}$ and $\sigma_{p_l}$ are the mean and the standard deviation of the input random variable $p_l$. Note that $\sigma_{p_l}$ is characterized by the measurement device accuracy, and $\mu_{p_l}$ depends on the actual system state.

2) *Evaluation of $\boldsymbol{F}(\cdot)$*: Each function $F_q(\cdot)$ is evaluated $2\eta$ times ($l = 1, \ldots, \eta; k = 1, 2$), yielding the vector $\boldsymbol{Y}(l,k)$, whose components $Y_q(l,k)$ are computed as

$$Y_q(l,k) = F_q(\mu_{p_1}, \ldots, \mu_{p_{l-1}}, p_{l,k}, \mu_{p_{l+1}}, \ldots, \mu_{p_\eta}) \ .$$

3) *Calculation of weights*: The weighting factors $w_{l,k}$ are computed as (see [25]):

$$w_{l,1} = \frac{1}{2\eta} \quad , \quad w_{l,2} = \frac{1}{2\eta} \ . \tag{8}$$

4) *Calculation of diagonal terms of $\boldsymbol{C}_{z,i}$*: Using the weights $w_{l,k}$ and the $Y_q(l,k)$ values, the $j$-th non-cross moment of the output random variable $y_q$ are estimated using (see [25]):

$$\mu^j_{Y_q} = E[Y_q^j] \approx \sum_{l=1}^{\eta}\sum_{k=1}^{2} w_{l,k}(Y_q(l,k))^j \ . \tag{9}$$

Note that the mean and the variance of the processed measurements can be easily computed from (9). For instance, the variance (second centered non-cross moment) of $P_{ij}$, $\sigma^2_{P_{ij}}$, is computed as

$$\sigma^2_{P_{ij}} = E[Y^2_{P_{ij}}] - E[Y_{P_{ij}}]^2 \ . \tag{10}$$

Therefore, the diagonal terms of $\boldsymbol{C}_{z,i}$ matrix are computed as the second centered non-cross moments of the output variable vector $\boldsymbol{y}$.

5) *Calculation of non-diagonal terms of $\boldsymbol{C}_{z,i}$*: The non-diagonal terms of $\boldsymbol{C}_{z,i}$ matrix are calculated as second centered cross moments. The second cross moments (between the output variables $y_q$ and $y_{q'}$) are computed as

$$c_{Y_qY_{q'}} = E[Y_qY_{q'}] \approx \sum_{l=1}^{\eta}\sum_{k=1}^{2} w_{l,k}(Y_q(l,k)Y_{q'}(l,k)) \ . \tag{11}$$

For instance, the second centered cross moment between the output random variables $V_i$ and $P_{ij}$, $c_{V_iP_{ij}}$, is calculated as

$$c_{V_iP_{ij}} = E[Y_{V_i}Y_{P_{ij}}] - E[Y_{V_i}]E[Y_{P_{ij}}] \ . \tag{12}$$

Applying the above method, a symmetric $\boldsymbol{C}_{z,i}$ matrix is obtained, as shown in (13) (see Page 5), where diagonal terms correspond to the variances of the processed measurements, and non-diagonal terms correspond to the products of the standard deviations with the correlation parameter between the corresponding variables. For instance, the term $c_{V_iP_i}$ corresponds to:

$$c_{V_iP_i} = \sigma_{V_i}\sigma_{P_i}\rho_{V_iP_i} \ . \tag{14}$$

Traditionally, matrix $\boldsymbol{C}_z$ is considered diagonal, and its inverse is used as the weighting matrix ($\boldsymbol{W}$) in the WLS estimator [10], providing a quantification of the precision of each measurement. In the proposed method, these "weights" are calculated analytically from the voltage/current/angle signal precisions.

The performance of the proposed method to calculate $\boldsymbol{C}_z$, based on a point estimate technique, has been carefully assessed comparing its results with those obtained using a numerical estimation of the measurement variance-covariance matrix. This assessment is based on a Monte Carlo algorithm: a set of independent Gaussian-distributed random vectors (representing the measurement samples of each input signal) have been generated and processed through (2)–(6) to obtain the corresponding dependent random vectors, which represent the output dependent processed measurements. Computing the variance-covariance matrix out of these vectors, a numerical estimation of $\boldsymbol{C}_z$ is obtained.

In order to derive statistically sound conclusions, sample sizes up to one million have been considered, and a sufficient number (up to ten thousands) of feasible operating points have been tested. The maximum relative error obtained between methods is smaller than $1\%$. It is thus concluded that the point estimate technique performs properly to estimate measurement variance-covariance matrices.

## III. Dependent State Estimation Model

Most state estimation models in practical use are formulated as overdetermined systems of non-linear equations of the form

$$\boldsymbol{z} = \boldsymbol{h}(\boldsymbol{x}^{\text{true}}) + \boldsymbol{e} \ , \tag{15}$$

where $\boldsymbol{z}$ is the vector of measurements, $\boldsymbol{x}^{\text{true}}$ is the true state vector, $\boldsymbol{h}(\cdot)$ is a non-linear function vector relating

measurements to states, and $\boldsymbol{e}$ is the measurement error vector with zero mean, which implies that meters are unbiased, i.e. $\mathrm{E}[\boldsymbol{e}] = 0$. There are $m$ measurements and $n$ state variables, $n < m$.

As stated in Section II, measurements are assumed to be dependent Gaussian distributed random variables, and their variance-covariance matrix is denoted as $\boldsymbol{C}_z$. From (15), note that the variance-covariance matrix of measurement errors is equal to $\boldsymbol{C}_z$ because $\boldsymbol{h}(\boldsymbol{x}^{\text{true}})$ is deterministic [12].

Considering that this paper focuses on measurement dependencies, our study relies on two traditional state estimation assumptions [10], namely:

1) Calibration is used to eliminate large systematical errors, and, thus, measurement errors are Gaussian and non-biased.
2) The exact network topology and the exact parameter values are known.

Note that the validity of these assumptions is analyzed in [26]–[30].

### A. State Estimation

Under the assumptions stated in the previous subsections, and once the measurement variance-covariance matrix $\boldsymbol{C}_z$ is obtained, the state estimation is performed as a Dependent Weighted Least Square (DWLS) problem that can be formulated mathematically as an optimization problem including equality and inequality constraints as follows:

$$\underset{\boldsymbol{x}}{\text{minimize}} \quad J = [\boldsymbol{z} - \boldsymbol{h}(\boldsymbol{x})]^T \boldsymbol{C}_z^{-1} [\boldsymbol{z} - \boldsymbol{h}(\boldsymbol{x})] \tag{16}$$

subject to

$$\boldsymbol{c}(\boldsymbol{x}) = \boldsymbol{0} \tag{17}$$

$$\boldsymbol{g}(\boldsymbol{x}) \leq \boldsymbol{0}\,, \tag{18}$$

where $\boldsymbol{x}$ is the state variable vector, $\boldsymbol{c}(\boldsymbol{x})$ are the equality constraints representing perfectly accurate measurements (zero injections), and $\boldsymbol{g}(\boldsymbol{x})$ are inequality constraints normally used to represent physical operating limits.

Note that the only difference with respect the traditional WLS formulation is that the variance-covariance matrix in (16) is non-diagonal.

The solution of problem (16)–(18), $\hat{\boldsymbol{x}}$, can be obtained by any of the efficient mathematical programming solvers (in terms of accuracy, required computing time and sparsity treatment) available nowadays [11], or, under certain assumptions with respect formulation (16)–(18), by any of the specific methods for solving the WLS problem proposed in the literature, [10].

Due to the nature of the variance-covariance matrix $\boldsymbol{C}_z$, composable by square blocks related to the buses along the matrix diagonal, its inverse can be calculated efficiently using the inverse of its blocks as follows:

$$\boldsymbol{C}_z^{-1} = \begin{pmatrix} \boldsymbol{C}_{z,1} \cdots & \boldsymbol{0} \\ \vdots \quad \ddots & \vdots \\ \boldsymbol{0} \quad \cdots & \boldsymbol{C}_{z,n} \end{pmatrix}^{-1} = \begin{pmatrix} \boldsymbol{C}_{z,1}^{-1} \cdots & \boldsymbol{0} \\ \vdots \quad \ddots & \vdots \\ \boldsymbol{0} \quad \cdots & \boldsymbol{C}_{z,n}^{-1} \end{pmatrix}. \tag{19}$$

Analogously, the Cholesky decomposition of the variance-covariance matrix $\boldsymbol{C}_z$ can be obtained through the Cholesky decompositions of their blocks.

### B. Bad Measurement Detection and Identification

The proposed DWLS method allows us to apply the traditional Chi-squares test in a simple manner. Note that the objective function (16) exhibits a $\chi^2$ distribution with at most $(m-n)$ degrees of freedom (see (28) in the Appendix). Thus, the $\chi^2$ test for detecting bad measurements can be used as detailed, for instance, in [10].

Bad measurement identification can be carried out through the normalized residual test, using the traditional approach, explained, for instance, in [10].

### C. Dependent State Estimation Algorithm

The algorithm to perform the dependent state estimation method proposed in this paper works as follows:

1) *Initial non-dependent estimation.* Assumptions stated in Section II imply that the variance-covariance matrix depends on the actual values of the state variables. As we do not know those values in advance, the traditional non-dependent estimation is used to get initial values of the positive sequence state variables $\hat{\boldsymbol{x}}^{(0)}$. The iteration counter is set to 1, $\nu = 1$.
Note that the weighting matrix used in the first estimation is diagonal, and it is computed using the meter variances (e.g., $0.01^2$ or $0.02^2$).

$$\boldsymbol{C}_{z,i} = \begin{array}{c} \\ V_i \\ P_i \\ Q_i \\ P_{ij} \\ \vdots \\ P_{ik} \\ Q_{ij} \\ \vdots \\ Q_{ik} \end{array} \begin{array}{c} \begin{array}{cccccccccc} V_i & P_i & Q_i & P_{ij} & \cdots & P_{ik} & Q_{ij} & \cdots & Q_{ik} \end{array} \\ \begin{pmatrix} \sigma^2_{V_i} & c_{V_iP_i} & c_{V_iQ_i} & c_{V_iP_{ij}} & \cdots & c_{V_iP_{ik}} & c_{V_iQ_{ij}} & \cdots & c_{V_iQ_{ik}} \\ c_{P_iV_i} & \sigma^2_{P_i} & c_{P_iQ_i} & c_{P_iP_{ij}} & \cdots & c_{P_iP_{ik}} & c_{P_iQ_{ij}} & \cdots & c_{P_iQ_{ik}} \\ c_{Q_iV_i} & c_{Q_iP_i} & \sigma^2_{Q_i} & c_{Q_iP_{ij}} & \cdots & c_{Q_iP_{ik}} & c_{Q_iQ_{ij}} & \cdots & c_{Q_iQ_{ik}} \\ c_{P_{ij}V_i} & c_{P_{ij}P_i} & c_{P_{ij}Q_i} & \sigma^2_{P_{ij}} & \cdots & c_{P_{ij}P_{ik}} & c_{P_{ij}Q_{ij}} & \cdots & c_{P_{ij}Q_{ik}} \\ \vdots & \vdots & \vdots & \vdots & \ddots & \vdots & \vdots & \ddots & \vdots \\ c_{P_{ik}V_i} & c_{P_{ik}P_i} & c_{P_{ik}Q_i} & c_{P_{ik}P_{ij}} & \cdots & \sigma^2_{P_{ik}} & c_{P_{ik}Q_{ij}} & \cdots & c_{P_{ik}Q_{ik}} \\ c_{Q_{ij}V_i} & c_{Q_{ij}P_i} & c_{Q_{ij}Q_i} & c_{Q_{ij}P_{ij}} & \cdots & c_{Q_{ij}P_{ik}} & \sigma^2_{Q_{ij}} & \cdots & c_{Q_{ij}Q_{ik}} \\ \vdots & \vdots & \vdots & \vdots & \ddots & \vdots & \vdots & \ddots & \vdots \\ c_{Q_{ik}V_i} & c_{Q_{ik}P_i} & c_{Q_{ik}Q_i} & c_{Q_{ik}P_{ij}} & \cdots & c_{Q_{ik}P_{ik}} & c_{Q_{ik}Q_{ij}} & \cdots & \sigma^2_{Q_{ik}} \end{pmatrix} \end{array} \tag{13}$$

2) *Variance-covariance matrix $\boldsymbol{C}_z^{(\nu)}$ calculation.* Per-phase values $V_i^f$, $I_{ij}^f$ and $\psi_{ij}^f$ are computed using the previous estimates $\hat{\boldsymbol{x}}^{(\nu-1)}$ and the following expressions:

$$\begin{aligned} V_i^f &= \hat{V}_i \quad \forall f \in \{A,B,C\} \\ I_{ij}^f &= \frac{\sqrt{\hat{P}_{ij}^{\,2} + \hat{Q}_{ij}^{\,2}}}{3\hat{V}_i} \quad \forall f \in \{A,B,C\} \\ \psi_{ij}^f &= \text{sign}(\hat{Q}_{ij}) \cos^{-1}\left(\frac{\hat{P}_{ij}}{\sqrt{\hat{P}_{ij}^{\,2} + \hat{Q}_{ij}^{\,2}}}\right) \\ &\quad \forall f \in \{A,B,C\}\ . \end{aligned} \tag{20}$$

From (20), note that the assumption of balanced operating conditions is used. The variance-covariance matrix approximation at iteration $\nu$, $\boldsymbol{C}_z^{(\nu)}$, is obtained using (a) these voltage, current, and phase angle values ($\mu_{p_l}, \forall p_l$), (b) standard deviation values for the corresponding voltage, current, and phase angle meters ($\sigma_{p_l}, \forall p_l$), and (c) the point-estimate method detailed in Section II-B.

3) *Dependent state estimation.* The state estimation problem considering dependencies (16)–(18) is solved using the approximation $\boldsymbol{C}_z^{(\nu)}$ of the variance-covariance matrix, and considering as initial values for the state variables those obtained in the previous iteration, $\hat{\boldsymbol{x}}^{(\nu-1)}$. The new estimates of the state variables correspond to $\hat{\boldsymbol{x}}^{(\nu)}$.

4) *Bad measurement detection.* Once the estimates $\hat{\boldsymbol{x}}^{(\nu)}$ are available, the Chi-squares test for bad measurement detection is performed. If bad measurement is suspected the algorithm continues in 5); else, if $||\hat{\boldsymbol{x}}^{(\nu)} - \hat{\boldsymbol{x}}^{(\nu-1)}|| > \varepsilon$ the estimation process continues in 2), otherwise, a solution within an $\varepsilon$ tolerance corresponds to $\hat{\boldsymbol{x}}^{(\nu)}$ and the algorithm concludes.

5) *Bad measurement identification.* Using the traditional method in [10], the bad measurement is identified and removed from the estimation process. The algorithm continues in 1).

Notwithstanding the iterative nature of the proposed algorithm, numerical studies show that just one iteration is needed, because matrix $\boldsymbol{C}_z^{(\nu)}$ does not change significantly from iteration to iteration.

### D. Estimation Assessment

In this section, the traditional WLS state estimator and the DWLS state estimation method, detailed in Section III-C, are compared. In order to carry out this comparison two sets of metrics are defined, $\text{MAE}_{\text{u},\omega}^{\text{WLS}}$ and $\text{MAE}_{\text{u},\omega}^{\text{DWLS}}$, which are measures of the quality of the WLS estimate and the DWLS estimate for each measurement scenario $\omega$, respectively. These measures are based on the Median Absolute Error (MAE) of a set of compared variables $\boldsymbol{u}$. Usually, the compared variables are $V_i$, $\theta_i$, $P_i$, $Q_i$ $\forall i$; $P_{ij}$, $Q_{ij}$ $\forall ij$; and $h_i(\boldsymbol{x})$ $\forall i$;.

These $\text{MAE}_{\text{u},\omega}$ expressions are

$$\text{MAE}_{\text{u},\omega}^{\text{WLS}} = \frac{\sum_{i=1}^{m_u} \left|\boldsymbol{u}^{\text{true}} - \boldsymbol{u}^{\text{WLS}}\right|}{m_u} \tag{21}$$

$$\text{MAE}_{\text{u},\omega}^{\text{DWLS}} = \frac{\sum_{i=1}^{m_u} \left|\boldsymbol{u}^{\text{true}} - \boldsymbol{u}^{\text{DWLS}}\right|}{m_u}\ , \tag{22}$$

where $m_u$ is the size of vector $\boldsymbol{u}$, and $\omega$ is the measurement scenario.

Once a sufficiently large number of state estimation simulations is performed, $\overline{\text{MAE}}_{\text{u}}$ is defined as the average $\text{MAE}_{\text{u},\omega}$ for all the considered scenarios $\omega$. Thus, for the WLS and DWLS estimation methods:

$$\overline{\text{MAE}}_{\text{u}}^{\text{WLS}} = \frac{\sum_{\omega=1}^{n_\omega} \text{MAE}_{\text{u},\omega}^{\text{WLS}}}{n_\omega} \tag{23}$$

$$\overline{\text{MAE}}_{\text{u}}^{\text{DWLS}} = \frac{\sum_{\omega=1}^{n_\omega} \text{MAE}_{\text{u},\omega}^{\text{DWLS}}}{n_\omega}\ , \tag{24}$$

where $n_\omega$ is the number of the considered scenarios.

Note that $\overline{\text{MAE}}_{\text{u}}$ represents the average absolute deviation between actual and estimated values for all the measurement scenarios $\omega$ considered (for the variable $\boldsymbol{u}$). Therefore, a method is comparatively more accurate than an alternative one with respect to $\boldsymbol{u}$ if its $\overline{\text{MAE}}_{\text{u}}$ is comparatively smaller.

Note also that the difference $\overline{\text{MAE}}_{\text{u}}^{\text{WLS}} - \overline{\text{MAE}}_{\text{u}}^{\text{DWLS}}$ represents the average $\boldsymbol{u}$-estimation improvement of using the DWLS method instead of the WLS one.

## IV. Generation of Measurements

To check the computational behavior of the DWLS method as compared with the traditional WLS one, we need to generate measurement scenarios with an actual dependence structure. The algorithm to generate those measurements proceeds as follows:

1) *Power flow solution.* The process starts from a given power flow solution that allows deriving the true state $\boldsymbol{x}^{\text{true}}$ (variables $V_i^{\text{true}}, \theta_i^{\text{true}}$ at every bus $i$). Therefore, $P_i^{\text{true}}, Q_i^{\text{true}}, P_{ij}^{\text{true}}$ and $Q_{ij}^{\text{true}}$ can be easily computed knowing the network data.

2) *True input measurement generation.* Assuming a sinusoidal balanced system state, true measurements $V_{f,i}^{\text{true}}$, $I_{f,ij}^{\text{true}}$ and $\psi_{f,ij}^{\text{true}}$ are calculated from the power flow solution through (20), using true values (based on $\boldsymbol{x}^{\text{true}}$).

3) *Actual measurement generation.* Adding an independent Gaussian-distributed error to the true values obtained in the previous step, actual input signals $V_i^f$, $I_{ij}^f$, and $\psi_{ij}^f$ are obtained:

$$\begin{aligned} V_i^f &= V_{f,i}^{\text{true}} + N(0,\sigma_V)\ , \\ I_{ij}^f &= I_{f,ij}^{\text{true}} + N(0,\sigma_I)\ , \\ \psi_{ij}^f &= \psi_{f,ij}^{\text{true}} + N(0,\sigma_\psi)\ . \end{aligned} \tag{25}$$

Using (2)–(6) and the actual input signals, dependent processed measurements ($V_i$, $P_i$, $Q_i$, $P_{ij}$, and $Q_{ij}$) are obtained.

In order to generate a set of dependent measurement scenarios based on the same power flow solution, note that only step 3) should be repeated.

## V. Case Studies

Two case studies are presented to illustrate the overall performance of the DWLS state estimation procedure presented

in this paper. In order to derive statistically sound conclusions a large number of state estimation problems up to five hundred is solved.

### A. 39-Bus Case Study

*1) DWLS Estimation:* In order to show the actual improvement of considering measurement dependencies in state estimation, the DWLS approach is applied to a 39-bus system [31]. Three-phase connection is considered for all the multi-function meters in the system, so that the formulation in Section II can be readily applied. The solution of an initial power flow is considered the true state, $\boldsymbol{x}^{\text{true}} = \{\boldsymbol{V}^{\text{true}}, \boldsymbol{\theta}^{\text{true}}\}$, and active/reactive power flow and injections are computed: $P_i^{\text{true}}$, $Q_i^{\text{true}}\ \forall i$; $P_{ij}^{\text{true}}$ and $Q_{ij}^{\text{true}}\ \forall ij$.

Assuming a sinusoidal balanced system state, $V_{f,i}^{\text{true}}$, $I_{f,ij}^{\text{true}}$ and $\psi_{f,ij}^{\text{true}}$ variables are calculated at each bus and line using (20). Afterwards, the $\boldsymbol{C}_z^{\text{true}}$ matrix is computed considering the measurement topology.

Table I provides the distribution of the absolute values of the correlation factors $\rho_{V_i,P_i}$, $\rho_{V_i,Q_i}$, $\rho_{P_i,Q_i}$ and $\rho_{P_{ij},Q_{ij}}$, for the 39-bus case study, computed from $\boldsymbol{C}_z^{\text{true}}$. Note that correlations are considerably high across different processed measurements, being inadequate the traditional assumption about null measurement correlations.

TABLE I
MEASUREMENT CORRELATIONS FOR THE 39-BUS CASE.

| Range of $\rho$ | $\lvert\rho_{V_i,P_i}\rvert$ (%) | $\lvert\rho_{V_i,Q_i}\rvert$ (%) | $\lvert\rho_{P_i,Q_i}\rvert$ (%) | $\lvert\rho_{P_{ij},Q_{ij}}\rvert$ (%) |
|---|---|---|---|---|
| $0.0 \leq \lvert\rho\rvert < 0.1$ | 41.90 | 61.17 | 7.63 | 6.15 |
| $0.1 \leq \lvert\rho\rvert < 0.2$ | 34.64 | 34.08 | 2.54 | 5.59 |
| $0.2 \leq \lvert\rho\rvert < 0.3$ | 9.22 | 2.23 | 2.54 | 4.75 |
| $0.3 \leq \lvert\rho\rvert < 0.4$ | 6.98 | 1.96 | 5.93 | 5.03 |
| $0.4 \leq \lvert\rho\rvert < 0.5$ | 2.23 | 0.00 | 2.54 | 3.63 |
| $0.5 \leq \lvert\rho\rvert < 0.6$ | 2.23 | 0.56 | 5.08 | 3.07 |
| $0.6 \leq \lvert\rho\rvert < 0.7$ | 1.12 | 0.00 | 0.85 | 6.15 |
| $0.7 \leq \lvert\rho\rvert < 0.8$ | 0.56 | 0.00 | 8.47 | 5.03 |
| $0.8 \leq \lvert\rho\rvert < 0.9$ | 1.12 | 0.00 | 12.71 | 11.73 |
| $0.9 \leq \lvert\rho\rvert \leq 1.0$ | 0.00 | 0.00 | 50.00 | 48.88 |

In order to illustrate the improvement achieved using the method proposed, two measurement configurations are studied: $r_1$ and $r_2$. Table II provides the number of voltage measurements, active/reactive power injection measurements and active/reactive power flow measurements considered for both measurement configurations. The last row in Table II provides the redundancy ratio (number of measurements divided by number of state variables).

Table III provides the structure of the $185 \times 185$ blocked matrix $\boldsymbol{C}_z$ for both measurement configurations. Note that $\boldsymbol{C}_z$ is a very sparse blocked matrix, as stated in Section III. This high degree of sparsity allows us to compute its inverse in an efficient way, using (19), Cholesky decomposition and parallel computation techniques.

For each measurement scenario, the state estimation algorithm is executed as follows: (i) initial non-dependent estimation (that is, traditional WLS estimation), (ii) $\boldsymbol{C}_z$ calculation, (iii) dependent state estimation, (iv) bad measurement detection and (v) bad measurement identification.

TABLE II
MEASUREMENT CONFIGURATIONS FOR THE CASE STUDIES.

| Type of measurement | 39-bus case study | | 118-bus case study | |
|---|---|---|---|---|
| | $r_1$ | $r_2$ | $r_1$ | $r_2$ |
| $V_i$ | 39 | 39 | 118 | 118 |
| $P_i$ | 10 | 27 | 54 | 110 |
| $Q_i$ | 10 | 27 | 54 | 110 |
| $P_{ij}$ | 46 | 46 | 179 | 179 |
| $Q_{ij}$ | 46 | 46 | 179 | 179 |
| Total | 151 | 185 | 584 | 696 |
| $r$ | 1.961 | 2.4026 | 2.4851 | 2.9617 |

TABLE III
STRUCTURE OF THE $\boldsymbol{C}_z$ MATRIX FOR THE CASE STUDIES.

| Block dimension | 39-bus case study | | 118-bus case study | |
|---|---|---|---|---|
| | $r_1$ | $r_2$ | $r_1$ | $r_2$ |
| $1 \times 1$ | 3 | 0 | 9 | 1 |
| $3 \times 3$ | 22 | 17 | 48 | 23 |
| $5 \times 5$ | 9 | 13 | 22 | 45 |
| $7 \times 7$ | 4 | 7 | 21 | 24 |
| $9 \times 9$ | 1 | 1 | 14 | 17 |
| $11 \times 11$ | 0 | 1 | 2 | 3 |
| $13 \times 13$ | 0 | 0 | 2 | 2 |
| Total | 39 | 39 | 118 | 118 |

Although the proposed algorithm is iterative (see Section III-C), it has been numerically established that only one iteration is required, because additional iterations make no substantial changes in matrix $\boldsymbol{C}_z$.

*2) 39-bus Single Scenario Analysis:* To compare initially both approaches a single measurement scenario is considered in this section, for the measurement configuration $r_2$.

Traditionally, WLS weighting matrix is generally computed as the inverse of the meter variance matrix $\boldsymbol{C}_z^{\text{trad}}$, whose diagonal terms are fixed values (e.g., $0.01^2$ for voltage magnitudes or $0.02^2$ for powers).

The measurement scenario is generated as detailed in Section IV. From Section V-A above, note that $\boldsymbol{C}_z^{\text{true}}$ can be computed, and, thus, the true meter variance diagonal matrix can be calculated as $\boldsymbol{C}_z^{\text{diag}} = \text{diag}(\boldsymbol{C}_z^{\text{true}})$.

Thus, the WLS estimation can be carried out using $\boldsymbol{C}_z^{\text{trad}}$ or $\boldsymbol{C}_z^{\text{diag}}$, obtaining different estimations: $\text{WLS}^{\text{trad}}$ and $\text{WLS}^{\text{diag}}$, respectively.

Figure 4 depicts a histogram of the absolute error for voltage estimations (magnitude and angle) obtained using the $\text{WLS}^{\text{trad}}$, $\text{WLS}^{\text{diag}}$, and DWLS methods. The vertical lines indicate $\text{MAE}_{\text{V}}$ and $\text{MAE}_{\theta}$ parameters for the three methods.

For this example, it can be concluded that the DWLS estimator outperforms clearly the traditional $\text{WLS}^{\text{trad}}$ one, obtaining an average absolute error about ten times smaller. On the other hand, the accuracy of the $\text{WLS}^{\text{diag}}$ estimator is between those of $\text{WLS}^{\text{trad}}$ and DWLS estimators.

Note that the differences between DWLS and $\text{WLS}^{\text{diag}}$ results are the consequence of considering or not dependencies, i.e., the effect of using a diagonal or a dense weighting matrix.

Since the DWLS estimator outperforms clearly the $\text{WLS}^{\text{trad}}$

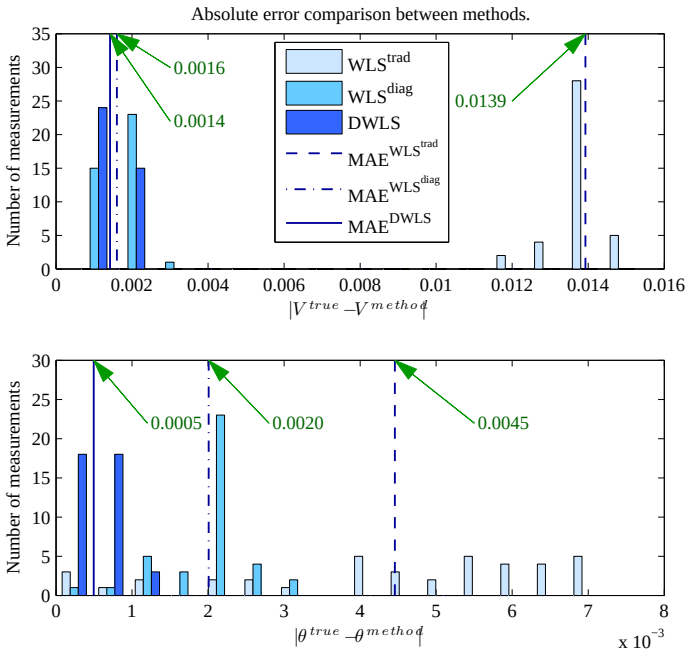


Fig. 4. Comparison between $\mathrm{WLS}^{\mathrm{trad}}$, $\mathrm{WLS}^{\mathrm{true}}$, and DWLS estimators.

one, in the following sections the compared estimators are the DWLS and the $\mathrm{WLS}^{\mathrm{diag}}$, the latter being called hereafter WLS.

*3) Multiple Measurement Scenario Comparison:* Five hundred state estimation scenarios are considered for this 39-bus case study. Each measurement scenario provides two sets of $\mathrm{MAE}_{\mathrm{u},\omega}$ values (one for the WLS estimation and other for the DWLS estimation), as stated in Section III-D. In order to compare $\mathrm{MAE}_{\mathrm{u},\omega}^{\mathrm{WLS}}$ and $\mathrm{MAE}_{\mathrm{u},\omega}^{\mathrm{DWLS}}$, six histograms are plotted in Fig. 5. These histograms represent five hundred measurement scenarios for the $r_2$ measurement configuration, and compare voltage magnitudes/angles, active/reactive power injections, active power flows and the functional vector $\boldsymbol{h}(\hat{\boldsymbol{x}})$. A vertical dashed line is plotted at $\mathrm{MAE}_{\mathrm{u},\omega}^{\mathrm{DWLS}} = \mathrm{MAE}_{\mathrm{u},\omega}^{\mathrm{WLS}}$.

Note that the dashed line in each histogram represents the case for which both methods exhibit the same average absolute estimation error. Note that the vast majority of the simulations lay on the right-hand side of the dashed line, which means that $\mathrm{MAE}_{\mathrm{u},\omega}^{\mathrm{WLS}}$ is larger than $\mathrm{MAE}_{\mathrm{u},\omega}^{\mathrm{DWLS}}$ for most of the cases.

Table IV provides the percentage of simulations for which the DWLS state estimation method provides a better average estimation than the traditional WLS method, and the $\overline{\mathrm{MAE}}_{\mathrm{u}}^{\mathrm{WLS}} - \overline{\mathrm{MAE}}_{\mathrm{u}}^{\mathrm{DWLS}}$ in % with respect to $\overline{\mathrm{MAE}}_{\mathrm{u}}^{\mathrm{WLS}}$ for each compared variable $\boldsymbol{u}$.

Note from Table IV that DWLS results slightly improve with a higher redundancy ratio $r$.

*4) Bad Measurement Detection with One Single Outlier:* In this subsection, WLS and DWLS bad measurement detection capabilities are studied and compared.

Five hundred additional measurement scenarios are generated, all of them populated with an outlier in one of the voltage magnitude signals (pre-processed measurements). Traditional WLS and DWLS estimations are run for each scenario, and the $\chi^2$ test is applied for both estimators. It is considered

TABLE IV
DWLS AND WLS ESTIMATION COMPARISON FOR THE 39-BUS CASE.

| Variable | Cases improved (%) | | $\frac{\overline{\mathrm{MAE}}_{\mathrm{u}}^{\mathrm{WLS}} - \overline{\mathrm{MAE}}_{\mathrm{u}}^{\mathrm{DWLS}}}{\overline{\mathrm{MAE}}_{\mathrm{u}}^{\mathrm{WLS}}}$ (%) | |
|---|---|---|---|---|
| | $r_1$ | $r_2$ | $r_1$ | $r_2$ |
| $V_i$ | 53.0 | 53.4 | 1.0 | 0.7 |
| $\theta_i$ | 80.2 | 80.0 | 39.2 | 39.9 |
| $P_i$ | 97.4 | 99.6 | 45.7 | 38.2 |
| $Q_i$ | 66.0 | 77.2 | 4.3 | 5.5 |
| $P_{ij}$ | 99.8 | 99.4 | 31.6 | 34.2 |
| $h_i(\hat{\boldsymbol{x}})$ | 99.6 | 99.6 | 19.9 | 22.0 |

that the measurement error is generated within the voltage measurement device, not in the multifunction meter (therefore, the error is spread among processed measurements in the same bus).

Numerical simulations show that if the bad measurement is a gross error or a extreme error (as defined in [32]), both methods detects this outlier with the same effectiveness:

- If the outlier standard deviation is larger than 6 times the measurement standard deviation, both techniques detects it with a high probability.
- A critical situation arises if the standard deviation ranges from 5 to 6 times the measurement standard deviation, because in some scenarios the bad measurement is not detected. However, both techniques behave in the same way.

Therefore, we conclude that the bad measurement detection capabilities of the DWLS estimator are similar to those of the traditional WLS estimator.

Note that cases involving multiple measurement gross errors are not studied in this paper. Multiple interacting bad measurements is a subject of future research.

### B. 118-Bus Case Study

In order to further analyze the actual performance of the DWLS estimator vs. the WLS one in a large power system, the IEEE 118-bus system [33] is considered.

Two measurement configurations $r_1$ and $r_2$ (detailed in Table II) are studied. Assuming a three-phase connection for all the multifunction meters and a sinusoidal balanced system state, the DWLS estimation algorithm explained in Section III-C is run for each measurement configuration and five hundred scenarios.

To appraise the computational burden of calculating $\boldsymbol{C}_z^{-1}$ in large systems, Table III provides the blocked structure of matrix $\boldsymbol{C}_z$.

Table V provides the percentage of simulations for which the DWLS state estimator outperforms the traditional WLS estimator, and the $\overline{\mathrm{MAE}}_{\mathrm{u}}^{\mathrm{WLS}} - \overline{\mathrm{MAE}}_{\mathrm{u}}^{\mathrm{DWLS}}$ in % with respect to $\overline{\mathrm{MAE}}_{\mathrm{u}}^{\mathrm{WLS}}$ for each compared variable $\boldsymbol{u}$. Note that the improvement percentages are significantly high and increase with the redundancy ratio $r$, attaining $100\%$ for several types of variables/measurements. Note that the $\overline{\mathrm{MAE}}_{\mathrm{u}}^{\mathrm{WLS}} - \overline{\mathrm{MAE}}_{\mathrm{u}}^{\mathrm{DWLS}}$ with respect to $\overline{\mathrm{MAE}}_{\mathrm{u}}^{\mathrm{WLS}}$ values slightly increase with the redundancy ratio $r$.

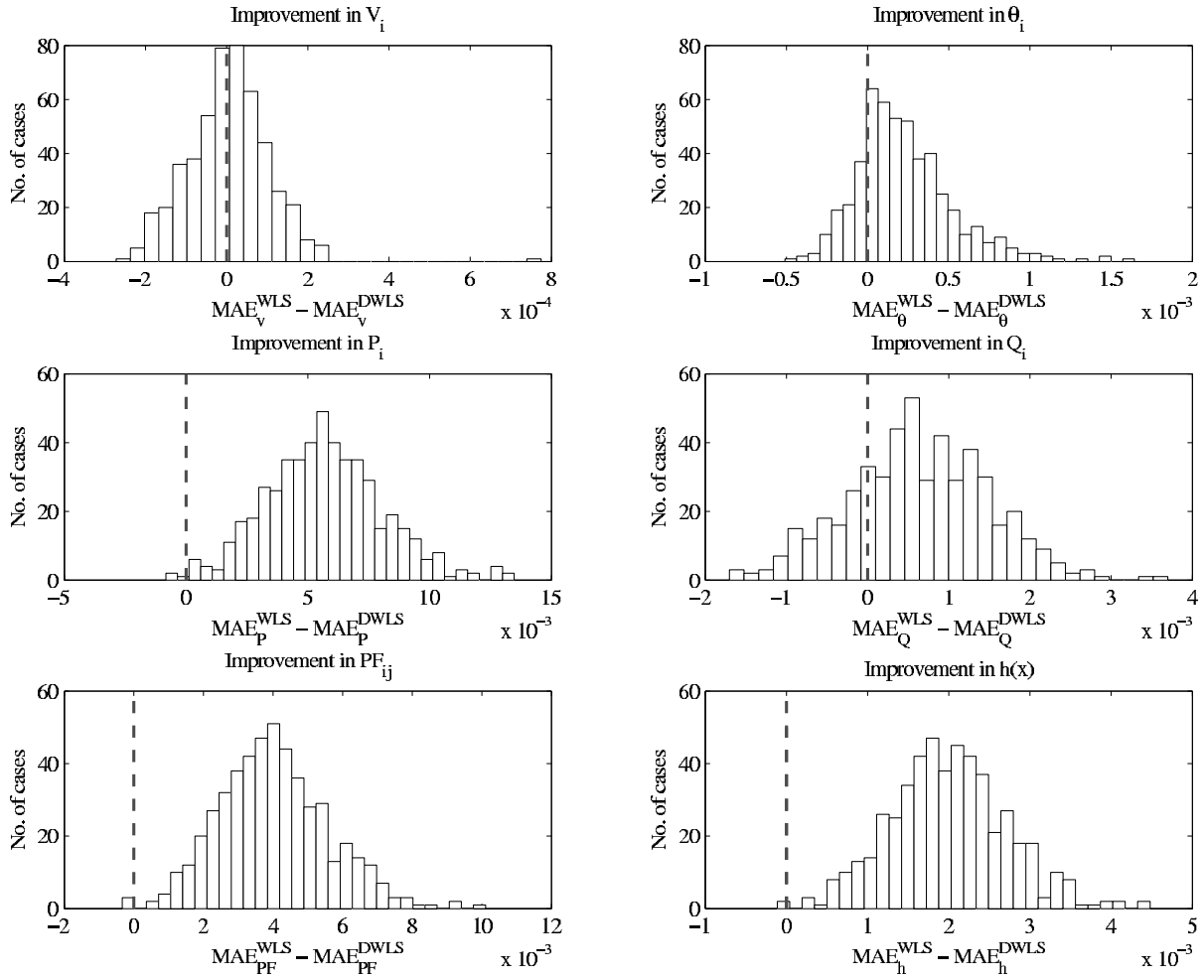


Fig. 5. Comparison of $\mathrm{MAE}_{\mathrm{u},\omega}^{\mathrm{WLS}}$ and $\mathrm{MAE}_{\mathrm{u},\omega}^{\mathrm{DWLS}}$ for the 39-bus case.

TABLE V
DWLS AND WLS ESTIMATION COMPARISON FOR THE 118-BUS CASE.

| Variable | Cases improved (%) | | $\frac{\overline{\mathrm{MAE}}_{\mathrm{u}}^{\mathrm{WLS}} - \overline{\mathrm{MAE}}_{\mathrm{u}}^{\mathrm{DWLS}}}{\overline{\mathrm{MAE}}_{\mathrm{u}}^{\mathrm{WLS}}}$ (%) | |
|---|---|---|---|---|
| | $r_1$ | $r_2$ | $r_1$ | $r_2$ |
| $V_i$ | 88.2 | 83.1 | 14.1 | 14.1 |
| $\theta_i$ | 88.8 | 91.2 | 27.9 | 36.5 |
| $P_i$ | 100 | 100 | 25.1 | 33.2 |
| $Q_i$ | 97.1 | 100 | 16.2 | 24.2 |
| $P_{ij}$ | 100 | 100 | 24.8 | 33.5 |
| $h_i(\hat{\boldsymbol{x}})$ | 100 | 100 | 22.2 | 29.9 |

Using MINOS [34] under GAMS [35] on a Linux-based server with four processors clocking at 2.6 GHz and 32 GB of RAM, the average computing time to perform a single WLS estimation is in this case study $0.55$ seconds, while a single DWLS estimation takes $0.55 + 0.87 = 1.42$ seconds. The computing time to perform the inversion of the matrix $\boldsymbol{C}_z$ of dimension $584 \times 584$ is $0.002849$ seconds.

### C. Case Study Conclusions

In the previous sections, both DWLS and WLS estimators have been studied and compared, in terms of accuracy and computational efficiency, for two realistic case studies.

Note that the DWLS estimator requires a greater computational effort than the traditional approach, but, considering current computers, this additional computational burden is not significant.

In terms of accuracy, Tables IV–V and Fig. 5 provide absolute and relative comparisons between both methods. Due to the inherent accuracy of the WLS estimator (if no gross errors affect the measurement set and if the weighting matrix corresponds to the inverse of the true variance diagonal matrix), providing a "much better" state estimate is practically impossible. For this reason, the absolute difference is small between methods (Fig. 5). Therefore, the most suitable comparison criterion is the relative one, provided in Tables IV–V. From these tables, note that the DWLS method clearly outperforms the WLS one, estimating always better any variable ($V_i$, $\theta_i$, $P_i$, $Q_i$, $P_{ij}$, or $h(\boldsymbol{x})$), and reaching relative improvements up to $45\%$.

## VI. CONCLUSION

Taking into account the actual measurement dependencies that occur within substations makes a difference in terms of estimation quality in power systems state estimation. This is

the main conclusion drawn from the analysis carried out and reported in this paper, which provides a technique to determine the measurement variance-covariance matrix (non-diagonal) and uses this matrix within a weighted least squares estimation procedure. Estimations using this dependent weighted least squares technique outperform statistically estimations obtained without considering existing measurement dependencies. This is shown using two realistic case studies.

Future research will focus on multiple gross errors detection and identification considering measurement dependencies. Particularly, the case of interacting and conforming multiple bad measurements will be considered.

## ACKNOWLEDGMENT

Authors are thankful to Juan M. Morales for insightful comments pertaining to point-estimate techniques.

## APPENDIX A
## ORTHOGONAL TRANSFORMATION OF NORMAL RANDOM VARIABLES

Let $\boldsymbol{e}$ be a correlated normal random error vector, with zero mean and variance-covariance matrix $\boldsymbol{C}_z$.

An uncorrelated random vector $\boldsymbol{u}$ and a linear transformation matrix $\boldsymbol{A}$ is sought, such that $\boldsymbol{u} = \boldsymbol{A}\boldsymbol{e}$.

The standard deviations of $\boldsymbol{C}_z$ should all be positive, because otherwise they have no physical meaning. This means that $\boldsymbol{C}_z$ should be a positive definite matrix, thus Cholesky decomposition can be applied, $\boldsymbol{C}_z = \boldsymbol{L}\boldsymbol{L}^T$.

To obtain an independent random vector $\boldsymbol{u}$ we need that its variance matrix $\boldsymbol{C}_u$ meets $\boldsymbol{C}_u = \boldsymbol{I}$, thus

$$\boldsymbol{C}_u = \boldsymbol{A}\boldsymbol{C}_z\boldsymbol{A}^T = (\boldsymbol{A}\boldsymbol{L})\left(\boldsymbol{L}^T\boldsymbol{A}^T\right) = \boldsymbol{I}. \tag{26}$$

For expression (26) to hold, $\boldsymbol{A}$ should be equal to $\boldsymbol{L}^{-1}$. This way matrix $\boldsymbol{A}$ is lower-triangular and $\boldsymbol{u}$ is a vector of standard independent normal random variables:

$$\boldsymbol{u} = \boldsymbol{A}\boldsymbol{e} = \boldsymbol{L}^{-1}\boldsymbol{e}. \tag{27}$$

Let us consider vector $\boldsymbol{e} = \boldsymbol{z} - \boldsymbol{h}(\boldsymbol{x}^{\text{true}})$ and the optimization problem (16)–(18). Using (27) the objective function in (16) becomes

$$\begin{aligned} J &= [\boldsymbol{z} - \boldsymbol{h}(\boldsymbol{x}^{\text{true}})]^T\boldsymbol{C}_z^{-1}[\boldsymbol{z} - \boldsymbol{h}(\boldsymbol{x}^{\text{true}})] \\ &= \boldsymbol{e}^T\left(\boldsymbol{L}\boldsymbol{L}^T\right)^{-1}\boldsymbol{e} = \boldsymbol{e}^T\left(\boldsymbol{L}^{-1}\right)^T\boldsymbol{L}^{-1}\boldsymbol{e} \\ &= \left(\boldsymbol{L}^{-1}\boldsymbol{e}\right)^T\boldsymbol{L}^{-1}\boldsymbol{e} = \boldsymbol{u}^T\boldsymbol{u}. \end{aligned} \tag{28}$$

The objective function $J$ above has a $\chi^2$ distribution because it is the sum of the squares of standard independent normal random variables $u_i \sim N(0, 1^2)$.

Using (27), note that problem (16) can be also expressed as a Least Squares (LS) problem:

$$\underset{\boldsymbol{x}}{\text{minimize}} \quad J = [\boldsymbol{L}^{-1}(\boldsymbol{z} - \boldsymbol{h}(\boldsymbol{x}))]^T[\boldsymbol{L}^{-1}(\boldsymbol{z} - \boldsymbol{h}(\boldsymbol{x}))]$$

subject to

$$\begin{aligned} \boldsymbol{c}(\boldsymbol{x}) &= \boldsymbol{0} \\ \boldsymbol{g}(\boldsymbol{x}) &\leq \boldsymbol{0}\,. \end{aligned}$$

## REFERENCES


[1] F. C. Schweppe and J. Wildes, "Power system static state estimation. Part I: Exact model," *IEEE Trans. Power App. Syst.*, vol. 89, no. 1, pp. 120–125, Jan. 1970.

[2] F. C. Schweppe and D. Rom, "Power system static state estimation. Part II: Approximate model," *IEEE Trans. Power App. Syst.*, vol. 89, no. 1, pp. 125–130, Jan. 1970.

[3] F. C. Schweppe, "Power system static state estimation. Part III: Implementation," *IEEE Trans. Power App. Syst.*, vol. 89, no. 1, pp. 130–135, Jan. 1970.

[4] R. Larson, W. Tinney, L. Hadju, and D. Piercy, "State estimation in power systems. part II: Implementations and applications," *IEEE Trans. Power App. Syst.*, vol. 89, no. 3, pp. 353–362, Mar. 1970.

[5] A. García, A. Monticelli, and P. Abreu, "Fast decoupled state estimation and bad data processing," *IEEE Trans. Power App. Syst.*, vol. 98, no. 5, pp. 1645–1652, Sept./Oct. 1979.

[6] A. Monticelli and A. García, "Fast decoupled state estimators," *IEEE Trans. Power Syst.*, vol. 5, no. 2, pp. 556–564, May 1990.

[7] J. J. Allemong, L. Radu, and A. M. Sasson, "A fast and reliable state estimation algorithm for AEP's new control center," *IEEE Trans. Power App. Syst.*, vol. 101, no. 4, pp. 933–944, Apr. 1982.

[8] L. Holten, A. Gjelsvik, S. Aam, F. Wu, and W. H. E. Liu, "Comparison of different methods for state estimation," *IEEE Trans. Power Syst.*, vol. 3, no. 4, pp. 1798–1806, Nov. 1988.

[9] A. Monticelli, "Electric power system state estimation," *Proceedings of the IEEE*, vol. 88, no. 2, pp. 262–282, 2000.

[10] A. Abur and A. G. Expósito, *Electric Power System State Estimation. Theory and Implementations*. New York: Marcel Dekker, 2004.

[11] E. Caro, A. J. Conejo, and R. Mínguez, "A mathematical programming approach to state estimation," in *Optimization Advances in Electric Power Systems*, E. D. Castronuovo, Ed. Nova Science Publishers, Inc., 2008.

[12] R. Mínguez, A. J. Conejo, and A. S. Hadi, "Non gaussian state estimation in power systems," in *Advances in Mathematical and Statistical Modeling*, ser. Statistics for Industry and Technology (SIT), B. C. Arnold, N. Balakrishnan, J. M. Sarabia, and R. Mínguez, Eds. Boston: Birkhauser.

[13] A. K. Ghosh, D. L. Lubkeman, M. J. Downey and R.H. Jones, "Distribution circuit state estimation using a probabilistic approach," *IEEE Trans. Power Syst.*, vol. 12, no. 4, pp. 45–51, Feb. 1997.

[14] A. K. Ghosh, D. L. Lubkeman and R.H. Jones, "Load modeling for distribution circuit state estimation," *IEEE Trans. Power Del.*, vol. 12, no. 2, pp. 999–1005, Apr. 1997.

[15] S. A. Molina, "Decomposition and measurement optimization in electrical power systems state estimation", Ph.D. Thesis, Imperial College of Science and Technology, University of London, Sept. 1977.

[16] *Multifunction Meter DM9200*, Td ed., Arteche, July 2005. Available on: *http://www.arteche.com/*.

[17] E. Rosenblueth, "Point estimates for probability moments," *Proc. Nat. Acad. Sci.*, vol. 72, pp. 3812–3814, Oct. 1975.

[18] ——, "Two-point estimates in probability," *Appl. Math. Model.*, vol. 5, pp. 329–335, Oct. 1981.

[19] S. S. Hyun and M. K. Byung, "Efficient statistical tolerance analysis for general distributions using three-point information," *Int. J. Prod. Res.*, vol. 40, no. 4, pp. 931–944, 2002.

[20] K. S. Li, "Point-estimate method for calculating statistical moments," *J. Eng. Mech.-ASCE* , vol. 118, no. 7, pp. 1506–1511, 1992.

[21] C. W. Tsai and S. Franceschini, "Evaluation of probabilistic point estimate methods in uncertainty analysis for environmental engineering applications," *J. Environ. Eng.-ASCE* , vol. 131, no. 3, pp. 387–395, 2005.

[22] W. Liping, D. Beeson, and G. Wiggs, "Efficient and accurate point estimate method for moments and probability distribution estimation," in *10th AIAA/ISSMO Multidisciplinary Analysis and Optimization Conference*, Albany, New York, 30 August-1 September 2004.

[23] M. E. Harr, "Probabilistic estimates for multivariate analysis," *Appl. Math. Model.*, vol. 13, no. 5, pp. 313–318, 1989.

[24] H. P. Hong, "An efficient point estimate method for probabilistic analysis," *Reliab. Eng. Syst. Saf.*, vol. 59, pp. 261–267, 1998.

[25] J. M. Morales and J. Pérez-Ruiz, "Point estimate schemes to solve the probabilistic power flow," *IEEE Trans. Power Syst.*, vol. 22, no. 4, pp. 1594–1601, Nov. 2007.

[26] K. A. Clements, and P. W. Davis "Detection and identification of topology errors in electric power systems," *IEEE Trans. Power Syst.*, vol. 3, pp. 1748, Nov. 1988.

[27] K. A. Clements,and A. Simões-Costa "Topology error identification using normalized Lagrange multipliers," *IEEE Trans. Power Syst.*, vol. 13, pp. 347353, May 1998.
[28] K. A. Clements,and A. Simões-Costa "Enhanced topology error processing via optimal measurement design," *IEEE Trans. Power Syst.*, vol. 23, no. 3, pp. 845-852, Aug. 2008.
[29] M. M. Adibi, and D. K. Thorne, "Remote measurement calibration," *IEEE Trans. on Power Systems*, Vol. PWRS-1, No. 2, May 1986, pp. 194-199.
[30] S. Zhong, and A. Abur, "Combined state estimation and measurement calibration," *IEEE Trans. Power Syst.*, vol. 20, pp. 458-465, 2005.
[31] M. A. Pai, *Energy Function Analysis for Power System Stability*. Boston: Kluwer Academic Publishers, 1989.
[32] H.-J. Koglin, T. Neisius, G. Beissler, and K. D. Schmitt, "Bad data detection and identification," *Electrical Power and Energy Systems*, vol. 12, no. 2, pp. 94–103, 1990.
[33] Power Systems Test Case Archive. Available on: *http://www.ee.washington.edu/research/pstca/*.
[34] A. Drud, "MINOS: A solver for large-scale nonlinear optimization problems." *The Solvers Manual.*, GAMS Development Corporation, Washington, DC, 2008.
[35] A. Brooke, D. Kendrick, A. Meeraus, R. Raman, and R. E. Rosenthal. *GAMS: a Users Guide*. Washington, DC: GAMS Development Corporation, 2008. Available on: *http://www.gams.com/*.

**Eduardo Caro** received from the Polytechnical University of Cataluña, Barcelona, Spain, the Electrical Engineering degree in June 2007. He is currently a Ph.D. student at the University of Castilla-La Mancha, Ciudad Real, Spain.

His research interests include power system state estimation, optimization, sensitivity analysis, and power system quality.

**Antonio J. Conejo** (F'04) received the M.S. degree from MIT, Cambridge, MA, in 1987, and a Ph.D. degree from the Royal Institute of Technology, Stockholm, Sweden in 1990. He is currently a full Professor at the Universidad de Castilla-La Mancha, Ciudad Real, Spain.

His research interests include control, operations, planning and economics of electric energy systems, as well as statistics and optimization theory and its applications.

**Roberto Mínguez** received from the University of Cantabria, Santander, Spain, the Civil Engineering degree, and the Ph.D. degree in Applied Mathematics and Computer Science in September 2000 and June 2003, respectively. During 2004 he worked as Visiting Scholar at Cornell University, New York, under the Fulbright program. He is currently an Assistant Professor of Numerical Methods in Engineering at the University of Castilla-La Mancha, Ciudad Real, Spain.

His research interests are reliability engineering, sensitivity analysis, numerical methods, and optimization.